

ARTICLE

Open Access

# Rv2346c enhances mycobacterial survival within macrophages by inhibiting TNF- $\alpha$ and IL-6 production via the p38/miRNA/NF- $\kappa$ B pathway

Jing Yao<sup>1</sup>, Xingran Du<sup>2</sup>, Sixia Chen<sup>1</sup>, Yan Shao<sup>3</sup>, Kaili Deng<sup>1</sup>, Mingzi Jiang<sup>4</sup>, Jingning Liu<sup>1</sup>, Ziyang Shen<sup>1</sup>, Xiaolin Chen<sup>5</sup> and Ganzhu Feng<sup>1</sup>

## Abstract

The intracellular survival of *Mycobacterium tuberculosis* (*Mtb*) has a central role in the pathogenesis of tuberculosis. *Mtb* Rv2346c is a member of 6-kDa early secreted antigenic target family of proteins, which are known to inhibit the host immune responses to promote bacillary persistence in macrophages. However, the mechanism through which Rv2346c participates in *Mtb* pathogenesis is unclear. In the present study, recombinant Rv2346c protein was synthesized and used to treat Bacillus Calmette–Guérin (BCG)-infected macrophages. The results showed that Rv2346c inhibited the proliferation of BCG-infected macrophages and enhanced the survival of BCG in macrophages. Tumor necrosis factor- $\alpha$  (TNF- $\alpha$ ) and interleukin (IL)-6 were upregulated during BCG infection but downregulated by Rv2346c. Additional experiments showed that nuclear transcription factor- $\kappa$ B (NF- $\kappa$ B) in BCG-infected macrophages induced the production of TNF- $\alpha$  and IL-6. In addition, miR-155 and miR-99b had a suppressive effect on NF- $\kappa$ B, and the expression of these miRNAs was promoted by p38. Furthermore, Rv2346c was shown to decrease the activation of NF- $\kappa$ B, whereas it enhanced the phosphorylation of p38 and the expression of miR-155 and miR-99b. The function of Rv2346c was also verified in *Mtb*-infected mice. The results showed that Rv2346c increased the observed bacterial load and lung injury and downregulated TNF- $\alpha$  and IL-6 in vivo. Overall, our results reveal that Rv2346c enhances mycobacterial survival in macrophages via inhibiting the production of TNF- $\alpha$  and IL-6 in a p38/miRNA/NF- $\kappa$ B pathway-dependent manner, suggesting that Rv2346c acts as a crucial virulence factor in *Mtb* infection and has potential use as a target for anti-tuberculosis therapy.

## Introduction

Tuberculosis (TB) remains a major public health problem worldwide, particularly in developing countries, and is caused by *Mycobacterium tuberculosis* (*Mtb*) infections. Approximately one-third of the world's population has been infected with *Mtb*<sup>1</sup>. Bacillus Calmette–Guérin

(BCG), a live-attenuated *Mycobacterium*, is the most widely used human vaccine against TB for controlling this common infection<sup>2</sup>. However, BCG is reported to partially protect against TB meningitis and disseminated TB in infants but not adequately protect against pulmonary TB, the most prevalent form of disease, in all age groups<sup>3</sup>. Therefore, gaining an understanding of the molecular mechanisms of the pathogenesis of TB is urgently needed to allow for more effective prophylaxis, diagnosis, and therapy.

*Mtb* is able to bind to phagocytic receptors after being inhaled, enter resident alveolar macrophages recruited

Correspondence: Ganzhu Feng (zhu1635253@163.com)

<sup>1</sup>Department of Respiratory Medicine, the Second Affiliated Hospital of Nanjing Medical University, Nanjing, Jiangsu 210011, China

<sup>2</sup>Department of Infectious Diseases, the Second Affiliated Hospital of Nanjing Medical University, Nanjing, Jiangsu 210011, China

Full list of author information is available at the end of the article.

© The Author(s) 2018



**Open Access** This article is licensed under a Creative Commons Attribution 4.0 International License, which permits use, sharing, adaptation, distribution and reproduction in any medium or format, as long as you give appropriate credit to the original author(s) and the source, provide a link to the Creative Commons license, and indicate if changes were made. The images or other third party material in this article are included in the article's Creative Commons license, unless indicated otherwise in a credit line to the material. If material is not included in the article's Creative Commons license and your intended use is not permitted by statutory regulation or exceeds the permitted use, you will need to obtain permission directly from the copyright holder. To view a copy of this license, visit <http://creativecommons.org/licenses/by/4.0/>.

from the bloodstream, and live in them as an intracellular pathogen. Macrophages act as the first line of immune defense against *Mtb* by clearing the pathogen and functioning as antigen-presenting cells, transforming *Mtb* antigens into immunogenic polypeptides and presenting them to T cells via the major histocompatibility complex to trigger adaptive immunity<sup>4</sup>. In the process of developing cellular immunity against *Mtb*, macrophages produce tumor necrosis factor- $\alpha$  (TNF- $\alpha$ ) through stimulation of Toll-like receptor-2 (TLR2)-mediated signaling pathway and translocation of nuclear transcription factor- $\kappa$ B (NF- $\kappa$ B) to the nucleus<sup>4,5</sup>. TNF- $\alpha$  further induces host cell apoptosis to promote clearance of *Mtb*<sup>6</sup>, which is related to the caspase 8-mediated extrinsic cell death pathway, involving apoptosis signal-regulating kinase 1, the mitogen-activated protein kinase (MAPK) p38, and c-Abl<sup>7</sup>. In response to *Mtb* infection, interleukin (IL)-6 is also produced to kill *Mycobacteria*<sup>8</sup>. Furthermore, microRNAs (miRNAs), which are capable of controlling the activity of protein-encoding genes, have been implicated in modulating molecular mechanisms of pathogenesis in *Mtb* infection<sup>9</sup>.

The virulence determinants that promote the intracellular survival of *Mtb* in macrophages is the pivotal issue regarding the pathogenesis of TB. *Mtb* is reported to exploit the 6 kDa early secreted antigenic target (ESAT-6) secretion system (ESX), which is responsible for exporting virulence factors and immunomodulators across the cytomembrane<sup>10</sup>. These ESX substrates are known to inhibit the host immune responses to promote bacillary persistence in macrophages and the 6 kDa early secretory antigenic target (ESAT-6) is one of those proteins secreted by ESX secretion system. *Mtb* exhibits membrane-perforating activity due to the secretion of ESAT-6<sup>11</sup>, which is responsible for the membrane rupture of phagosomes and the subsequent escape of *Mtb* into the cytoplasm<sup>12</sup>. The ESAT-6-encoding gene is located in the RD1 region, which is conserved in virulent *Mycobacterium bovis* and *Mtb* strains, and is deleted from all BCG substrains<sup>13</sup>. It has been shown that *Mtb* Rv2346c (Gene ID: 888956) is a member of the ESAT-6-like family of proteins; thus, it may possess some common functions with ESAT-6. As Rv2346c also displays some differences with other family members, it may function differently in some respects. The overexpression of Rv2346c in *Mtb* has been reported to enhance its survival in human and mouse macrophages by inducing oxidative stress-mediated genomic instability<sup>14</sup>. However, the role of Rv2346c in *Mtb* pathogenesis and host immunity is still unclear. In this study, recombinant Rv2346c protein was produced to evaluate its immunomodulatory effect on BCG-infected macrophages and the related molecular mechanism. The function of Rv2346c was also verified in vivo.

## Results

### Heterologous expression and purification of recombinant Rv2346c

The Rv2346c protein was synthesized and purified for further investigation. The Rv2346c-encoding gene was amplified by PCR, cloned into the plasmid pET-30a(+), and transformed into *Escherichia coli* BL21 (DE3). The positive clones were confirmed by sequencing, the results of which are shown in Fig S1a. The recombinant protein Rv2346c was expressed in *E. coli* BL21(DE3) and was subsequently purified with Ni-IDA resin.

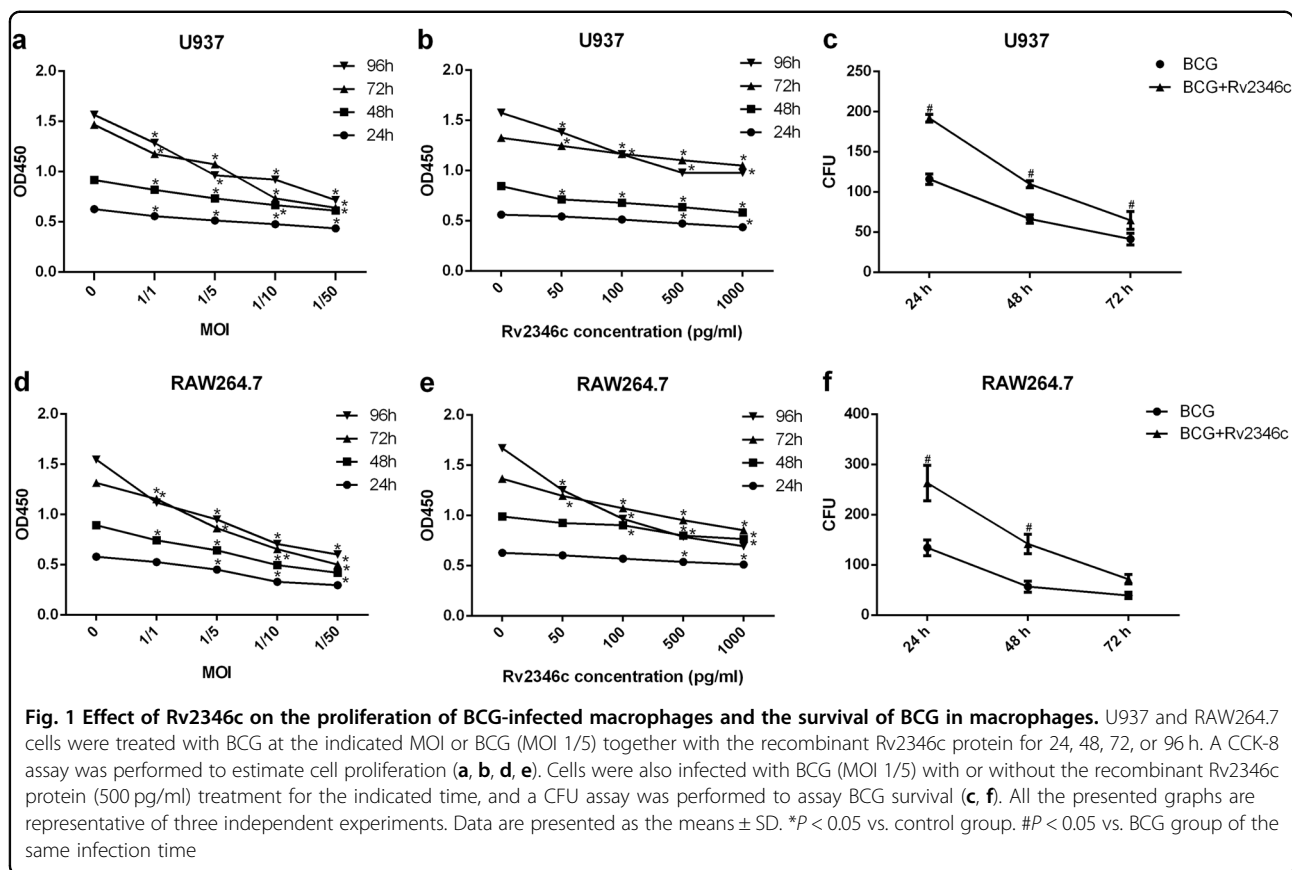
### Rv2346c inhibits the proliferation of BCG-infected macrophages and enhances the survival of BCG in macrophages

To explore the function of Rv2346c in TB, a cell counting kit-8 (CCK-8) assay was used to estimate its effect on BCG-infected macrophage proliferation. The results demonstrated that BCG infection significantly inhibited U937 and RAW264.7 cell proliferation, and this effect increased with higher multiplicity of infections (MOIs) of BCG and longer incubation times (Fig. 1a, d). When U937 and RAW264.7 cells were treated with BCG and Rv2346c simultaneously, Rv2346c further inhibited cell proliferation in a dose-dependent manner (Fig. 1b, e), whereas Rv2346c alone did not affect cell proliferation (Fig S1b, c). Macrophages have been reported to be capable of phagocytosing and killing *Mtb*. In the present study, the survival of BCG in U937 and RAW264.7 cells was evaluated by a colony-forming unit (CFU) assay. Our results showed that Rv2346c inhibited the germicidal efficacy of U937 and RAW264.7 cells and enhanced the survival of BCG (Fig. 1c, f).

### Rv2346c inhibition of cytokine production is accompanied by the downregulation of p65 and upregulation of p38 phosphorylation in BCG-infected macrophages

TNF- $\alpha$  and IL-6 participate in the clearance of *Mtb* by macrophages<sup>15,16</sup>. To determine whether Rv2346c impaired the germicidal efficacy of macrophages by decreasing the production of these cytokines, the TNF- $\alpha$  and IL-6 levels in cell culture supernatants were evaluated by enzyme-linked immunosorbent assay (ELISA). The results showed that TNF- $\alpha$  and IL-6 levels in supernatants were increased after BCG infection in U937 and RAW264.7 cells, whereas these increases were inhibited by the addition of Rv2346c (Fig. 2a–d). These data indicated that Rv2346c enhanced the survival of BCG by inhibiting the production of TNF- $\alpha$  and IL-6.

The production of TNF- $\alpha$  and IL-6 have been reported to be induced by NF- $\kappa$ B activation in macrophages, which can be evaluated by assessing the level of p65, a NF- $\kappa$ B subunit<sup>17,18</sup>. Our results also showed that the expression of p65 is in line with the observed p65 phosphorylation,



which supports NF- $\kappa$ B activation, during BCG infection, Rv2346c treatment, p65 overexpression, or p65 interference (Figs S2 and S3). In addition, p38 is known to affect proinflammatory cytokines in *Mtb*-infected macrophages and its activity can be estimated by its phosphorylation level<sup>19</sup>. To identify the upstream regulator of these cytokines that is affected by Rv2346c, the protein expression levels of p65 and p-p38 were evaluated by western blotting and the mRNA level of p65 was assessed by quantitative reverse-transcription PCR (qRT-PCR). The results showed that transcription and translation of p65 were upregulated in BCG-infected macrophages, but this effect was reduced after cells were treated with Rv2346c (Fig. 2e, f, h, i, j, l). In addition, BCG infection upregulated the level of p38 phosphorylation in macrophages, which was further enhanced by treating cells with Rv2346c (Fig. 2e, g, i, k). These data suggested that NF- $\kappa$ B and p38 participated in the Rv2346c-mediated regulation of cytokine expression in BCG-infected macrophages.

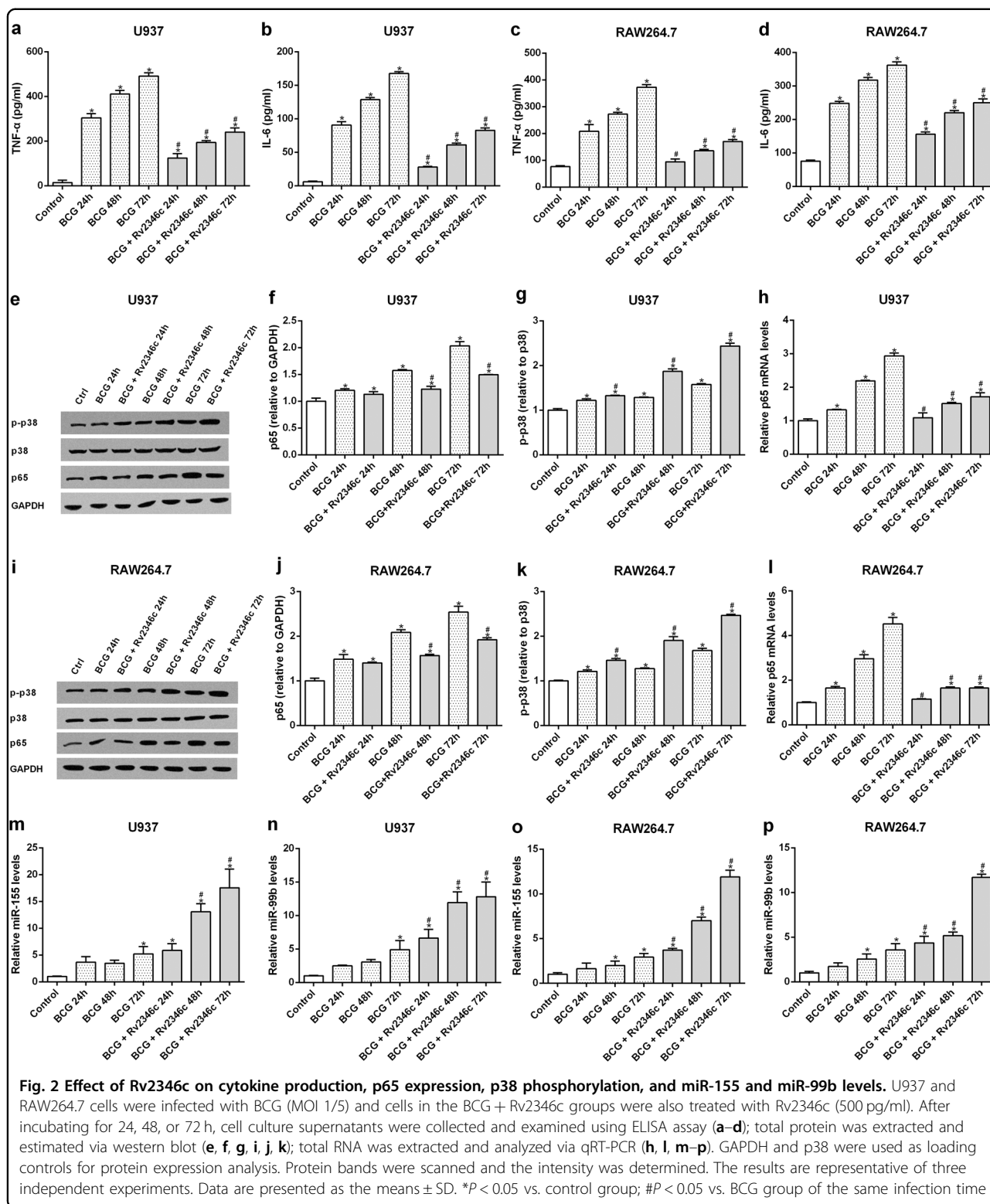
#### Rv2346c upregulates miR-155 and miR-99b in BCG-infected macrophages

The expressions of numerous proteins are regulated by miRNAs in eukaryotes. To identify miRNAs associated with the process of BCG infection, a microarray analysis

was conducted to miRNAs that were differentially expressed between the BCG-infected and BCG + Rv2346c groups. We detected 2006 miRNAs in U937 cells and 1193 miRNAs in RAW264.7 cells. Differentially expressed miRNAs were identified using a screening criterion of  $|\text{Fold change}| \geq 2$  and identified miRNAs are shown in Fig S4. Among these, miR-155 and miR-99b were significantly upregulated in Rv2346c-treated cells and these miRNAs have been previously observed to be associated with *Mtb* infection. The expression levels of miR-155 and miR-99b in U937 and RAW264.7 cells were evaluated by qRT-PCR. The results showed that BCG infection upregulated the levels of miR-155 and miR-99b in U937 and Raw264.7 cells, which was further enhanced by treatment with Rv2346c (Fig. 2m–p).

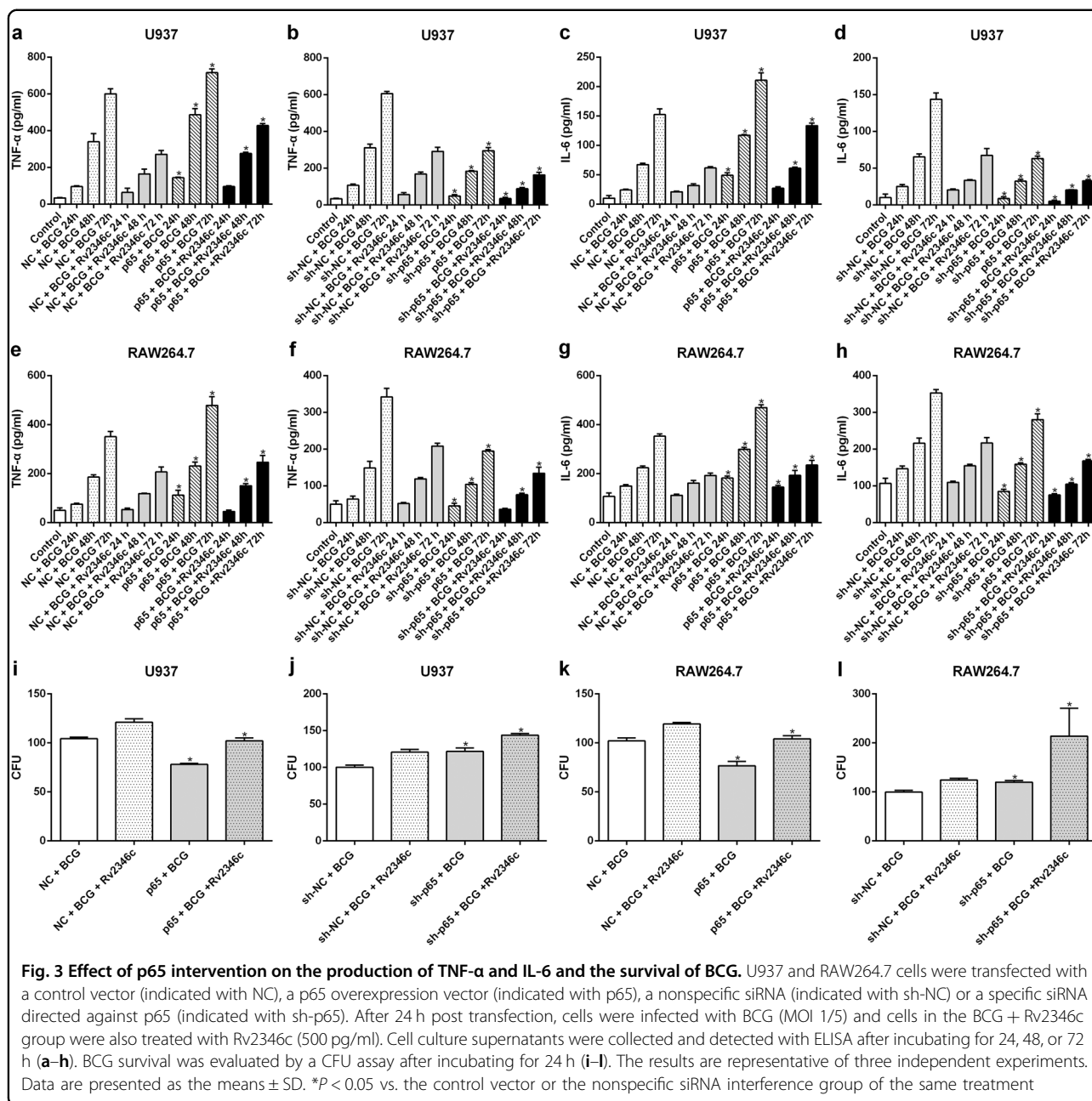
#### p65 upregulates the levels of TNF- $\alpha$ and IL-6 without affecting p38 phosphorylation and miRNA expression

To verify the effect of p65 on cytokine regulation in *Mtb* infection, p65 was upregulated in U937 and RAW264.7 cells via transfection with pcDNA3.1/p65 cDNA or downregulated through transfection with a specific small interfering RNA (siRNA) directed against p65. The efficacy of the treatments was evaluated by western blotting and qRT-PCR analyses (Fig S5). The result showed that



p65 overexpression upregulated TNF-α and IL-6 expression, whereas p65 interference significantly reduced the levels of TNF-α and IL-6 (Fig. 3a–h). In addition, overexpression of p65 enhanced the germicidal effect against

BCG, whereas downregulation of p65 suppressed the bactericidal activity of macrophages against BCG, which was in line with its observed regulation of cytokine production (Fig. 3i–l). These results did not indicate the



existence of a regulatory effect of p65 on the phosphorylation of p38 (Fig S6) or the expression of miR-155 and miR-99b (Fig S7).

#### miR-155 and miR-99b downregulate the expression of p65 and the levels of TNF- $\alpha$ and IL-6 without affecting p38 phosphorylation

As miR-155 and miR-99b were observed to be upregulated in BCG-infected macrophages, especially when Rv2346c was added, we hypothesized that they regulate NF- $\kappa$ B activation or p38 phosphorylation. Therefore, U937 and RAW264.7 cells were transfected with miR-155

or miR-99b mimics or with miR-155 or miR-99b inhibitors to evaluate their potential regulatory activities (Fig S8). The results showed that both miR-155 and miR-99b downregulated the expression of p65, and this effect was enhanced by their combined activity (Fig. 4a–d). When miR-155 and miR-99b were knocked down, the level of p65 was upregulated (Fig. 4e–h). Neither miR-155 nor miR-99b had an effect on p38 phosphorylation (Fig S9). This finding suggested that miR-155 and miR-99b function as negative regulators upstream of p65 but act downstream of p38 or had no obvious relationship with p38. To verify the hypothesis, the relationship

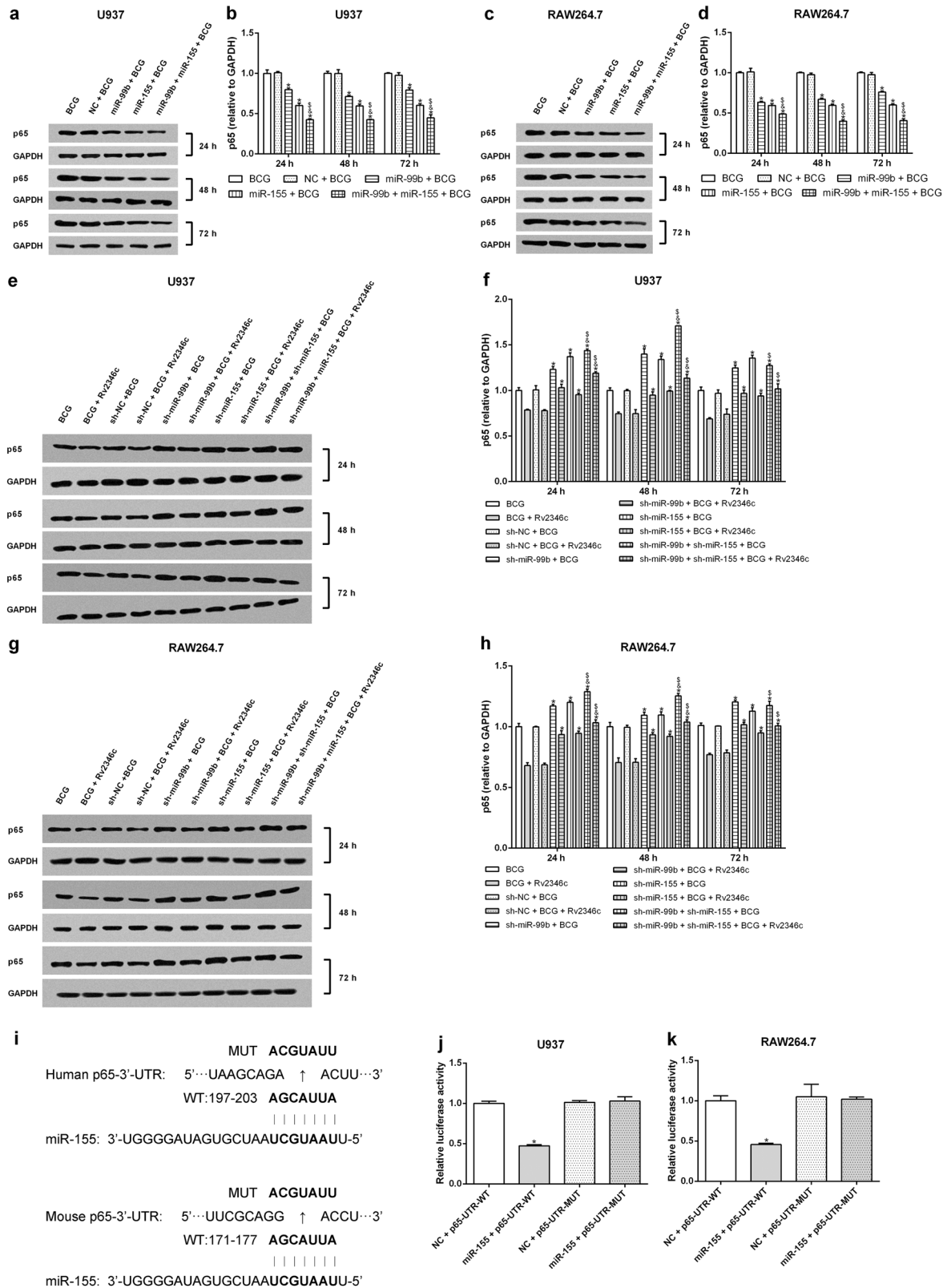


Fig. 4 (See legend on next page.)

(see figure on previous page)

**Fig. 4 Effect of miR-155 and miR-99b on p65 expression.** U937 and RAW264.7 cells were transfected with a negative control miRNA mimic (indicated with NC), miR-155, or miR-99b mimics, both miR-155 and miR-99b mimics, a negative control miRNA inhibitor (indicated with sh-NC), a miR-155 inhibitor (indicated with sh-miR-155), a miR-99b inhibitor (indicated with sh-miR-99b), or both the miR-99b and miR-155 inhibitors. After 24 h post transfection, cells were infected with BCG (MOI 1/5) and cells in the BCG + Rv2346c group were also treated with Rv2346c (500 pg/ml). After incubating for 24, 48, or 72 h, cells were collected to extract total protein. The protein expression was detected via western blotting. The results are representative of three independent experiments. Data are presented as the means  $\pm$  SD. \* $P < 0.05$  vs. a negative control (NC group or sh-NC group) + BCG group (with or without Rv2346c treatment); &#x26;#x2013; $P < 0.05$  vs. miR-99b or sh-miR-99b + BCG group (with or without Rv2346c treatment); \$ $P < 0.05$  vs. miR-155 or sh-miR-155 + BCG group (with or without Rv2346c treatment) (a–h). Sequence alignment of miR-155 and its conserved target site in the P65-UTR is shown (i). Luciferase activity was measured in U937 and RAW264.7 cells with a dual-luciferase reporter assay. The cells were co-transfected with a plasmid expressing miR-155 mimic or a control miRNA (indicated with NC) and a vector expressing P65-UTR WT or P65-UTR MUT. Firefly luciferase activity was normalized to *Renilla* luciferase activity. The results are representative of three independent experiments. Data are presented as the means  $\pm$  SD. \*  $P < 0.05$  vs. NC + P65-UTR-WT group (j, k)

between miRNAs (miR-155 and miR-99b) and p65 was analyzed using Miranda. The P65-UTR sequence was observed to contain a binding site for miR-155 but not for miR-99b (Fig. 4i). A dual-luciferase reporter assay was subsequently performed to verify the interaction between miRNAs (miR-155 and miR-99b) and p65. The results showed that miR-155 suppress luciferase expression, whereas miR-99b did not affect the luciferase expression significantly. Once the putative binding site is mutated, miR-155 failed to significantly downregulate the expression of luciferase (Fig. 4j, k and Fig S10). These findings indicated that a miR-155-binding site was present in the P65-UTR, and that miR-155 directly downregulated the expression of p65. The binding was specific, because the luciferase expression was not affected by the control miRNA.

To confirm the relationship between these miRNAs and p65, the effect of miR-155 and miR-99b on cytokine production was investigated. The results suggested that both miR-155 and miR-99b inhibited TNF- $\alpha$  and IL-6 production when overexpressed, and this effect was enhanced during their simultaneous overexpression. Knockdown of miR-155 and miR-99b upregulated TNF- $\alpha$  and IL-6 production, but this effect was not augmented when they were simultaneously knocked down (Fig. 5). This finding is in accordance with the impact of p65 on cytokine production, indicating that miR-155 and miR-99b negatively regulate p65, affecting cytokine production.

#### p38 regulates miRNA expression, p65 level, and cytokine production

To identify the function of p38 in BCG-infected macrophages, U937 and RAW264.7 cells were transfected with pcDNA3.1/p38 cDNA or a specific siRNA directed against p38. The modified expression of p38 was verified by western blotting (Fig S11). The results showed that overexpression of p38 resulted in upregulation of miR-155 and miR-99b, and decreased the level of p65. In

addition, knockdown of p38 caused the downregulation of miR-155 and miR-99b expression, and increased that of p65 (Fig. 6a–h). Overexpression of p38 also had a suppressive role on the production of TNF- $\alpha$  and IL-6. In contrast, knockdown of p38 upregulated the levels of TNF- $\alpha$  and IL-6 (Fig. 6i–l). These data indicated that Rv2346c enhanced BCG survival in macrophages via the p38/miRNA/NF- $\kappa$ B pathway.

#### Rv2346c enhances the virulence of *Mtb* and inhibits the production of TNF- $\alpha$ and IL-6 in vivo

To verify the function of Rv2346c in *Mtb* infection, C57BL/6 mice were intratracheally infected with the *Mtb* strains H37Rv, H37Ra,  $\Delta$ Rv2346c, or  $\Delta$ Rv2346c/ $\Delta$ Rv2346c::pMV261. The mouse mortality was observed for 55 days post infection (dpi), after which the mice were killed to obtain the lungs. Notably,  $\Delta$ Rv2346c-treated C57BL/6 mice showed a much lower mortality than the H37Rv- and  $\Delta$ Rv2346c/ $\Delta$ Rv2346c::pMV261-treated mice (Fig. 7a). In agreement with the corresponding survival curves, the bacterial load of  $\Delta$ Rv2346c-treated C57BL/6 mice was much lower than those observed for H37Rv- and  $\Delta$ Rv2346c/ $\Delta$ Rv2346c::pMV261-treated mice (Fig. 7b). Thus, the data demonstrated that Rv2346c augmented the virulence of *Mtb* in vivo. The lung tissues were collected at 35 dpi to observe *Mtb*-induced damage. Numerous inflammatory foci were observed in *Mtb*-infected lung parenchyma, except in mice treated with BCG (Fig. 7d–i). Histological lesions exhibited epithelioid and foamy macrophages and neutrophil clustering, as well as numerous islands of karyorrhectic debris surrounded by epithelioid macrophages and some multinucleated giant cells. Morphometric analysis of hematoxylin and eosin (H&E)-stained histological sections revealed that the lungs of  $\Delta$ Rv2346c-treated C57BL/6 mice were less injured than those of the H37Rv- and  $\Delta$ Rv2346c/ $\Delta$ Rv2346c::pMV261-treated mice (Fig. 7c).

Immunofluorescence analyses confirmed that mice treated with H37Rv and  $\Delta$ Rv2346c showed increasing

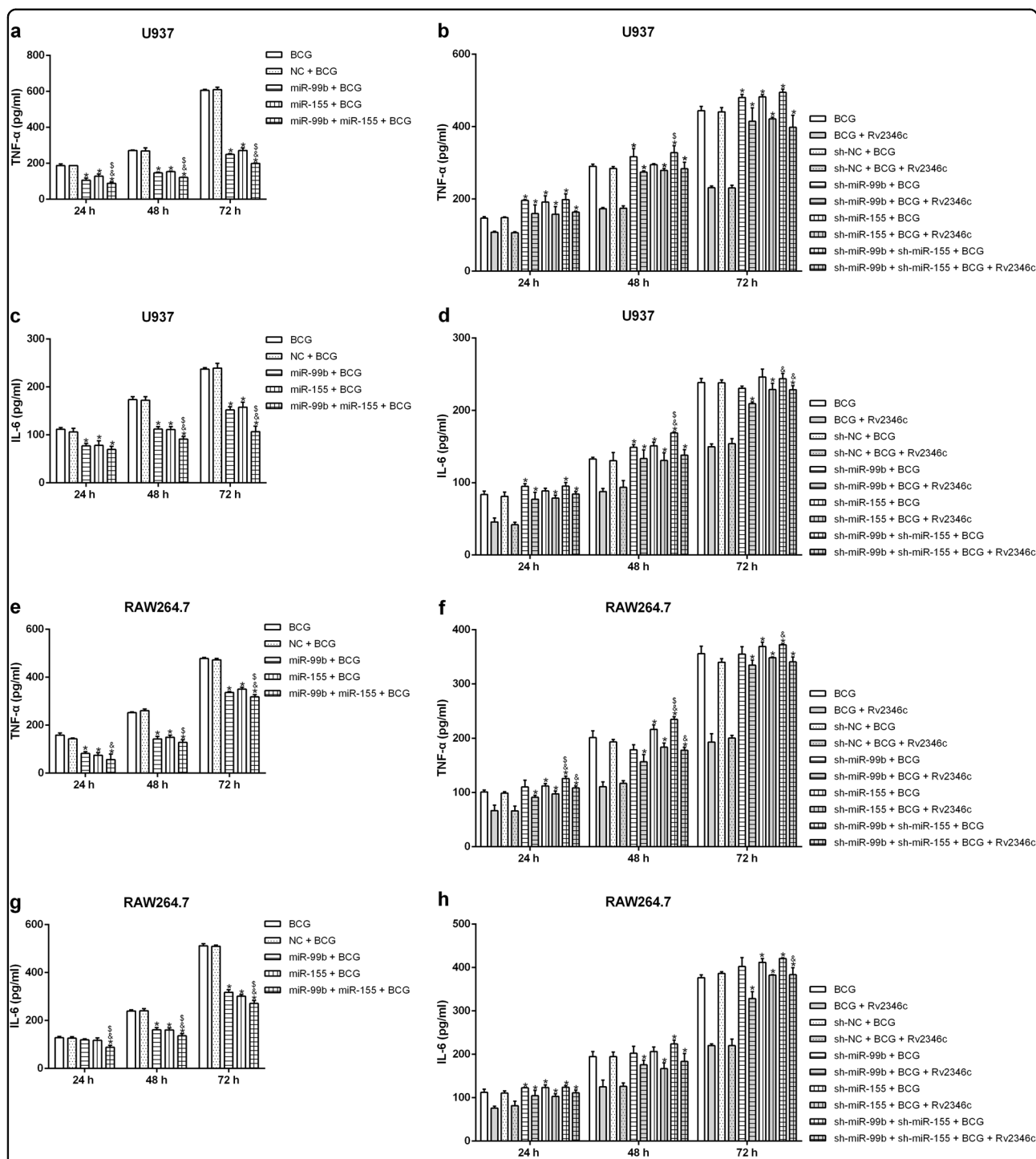
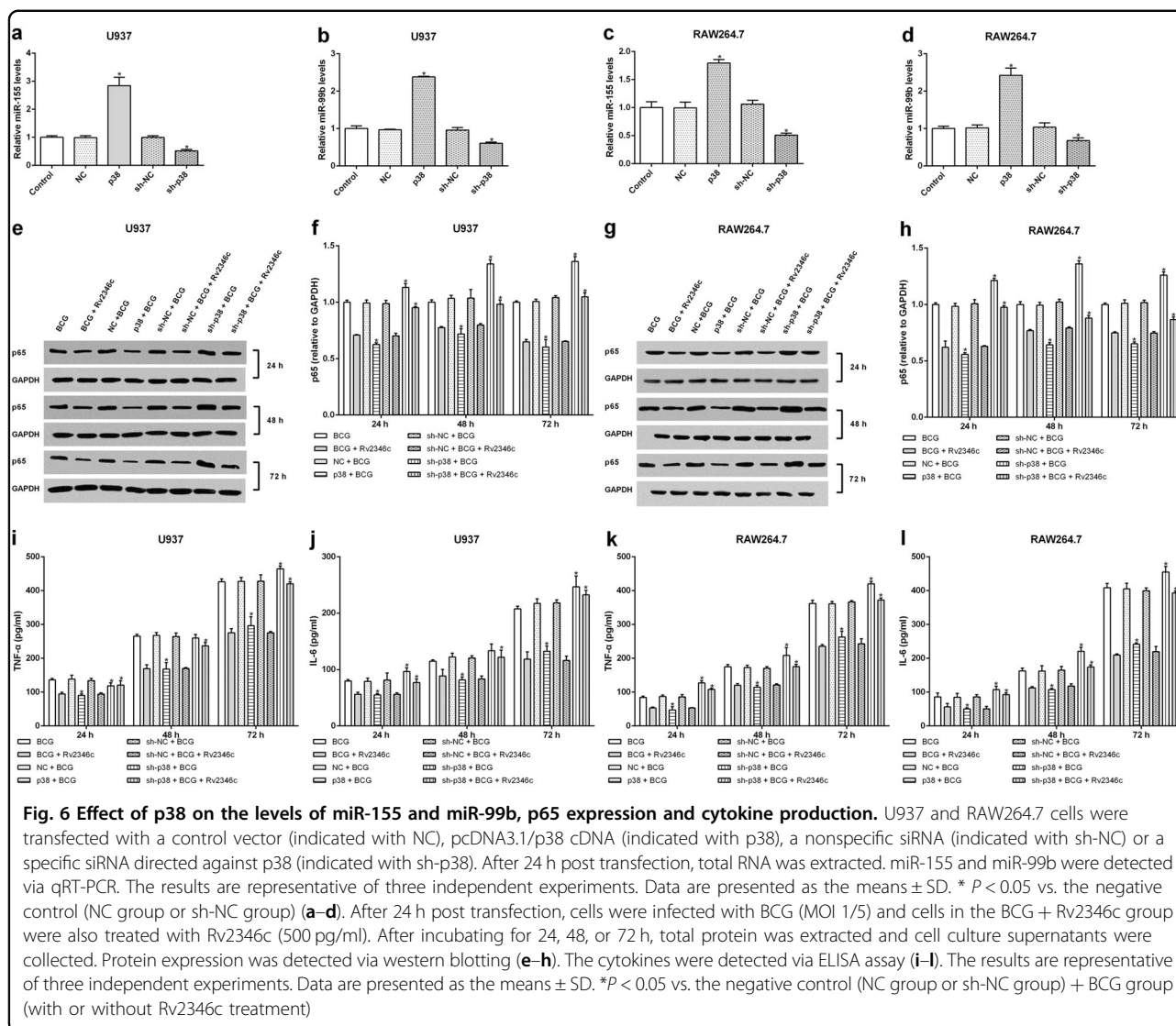


**Fig. 5** Effect of miR-155 and miR-99b on the production of TNF- $\alpha$  and IL-6. U937 and RAW264.7 cells were transfected with a negative control miRNA for mimic (indicated with NC), miR-155, or miR-99b mimics, both miR-155 and miR-99b mimics, a negative control miRNA inhibitor (indicated with sh-NC), a miR-155 inhibitor (indicated with sh-miR-155), a miR-99b inhibitor (indicated with sh-miR-99b), or both the miR-155 and miR-99b inhibitors. After 24 h post transfection, cells were infected with BCG (MOI 1/5) and cells in the BCG + Rv2346c group were also treated with Rv2346c (500 pg/ml). After incubating for 24, 48, or 72 h, cell culture supernatants were collected and detected with ELISA assay. The results are representative of three independent experiments. Data are presented as the means  $\pm$  SD. \* $P < 0.05$  vs. the negative control (NC group or sh-NC group) + BCG group (with or without Rv2346c treatment); &P  $< 0.05$  vs. miR-99b/sh-miR-99b + BCG group (with or without Rv2346c treatment); \$P  $< 0.05$  vs. miR-155/sh-miR-155 + BCG group (with or without Rv2346c treatment)





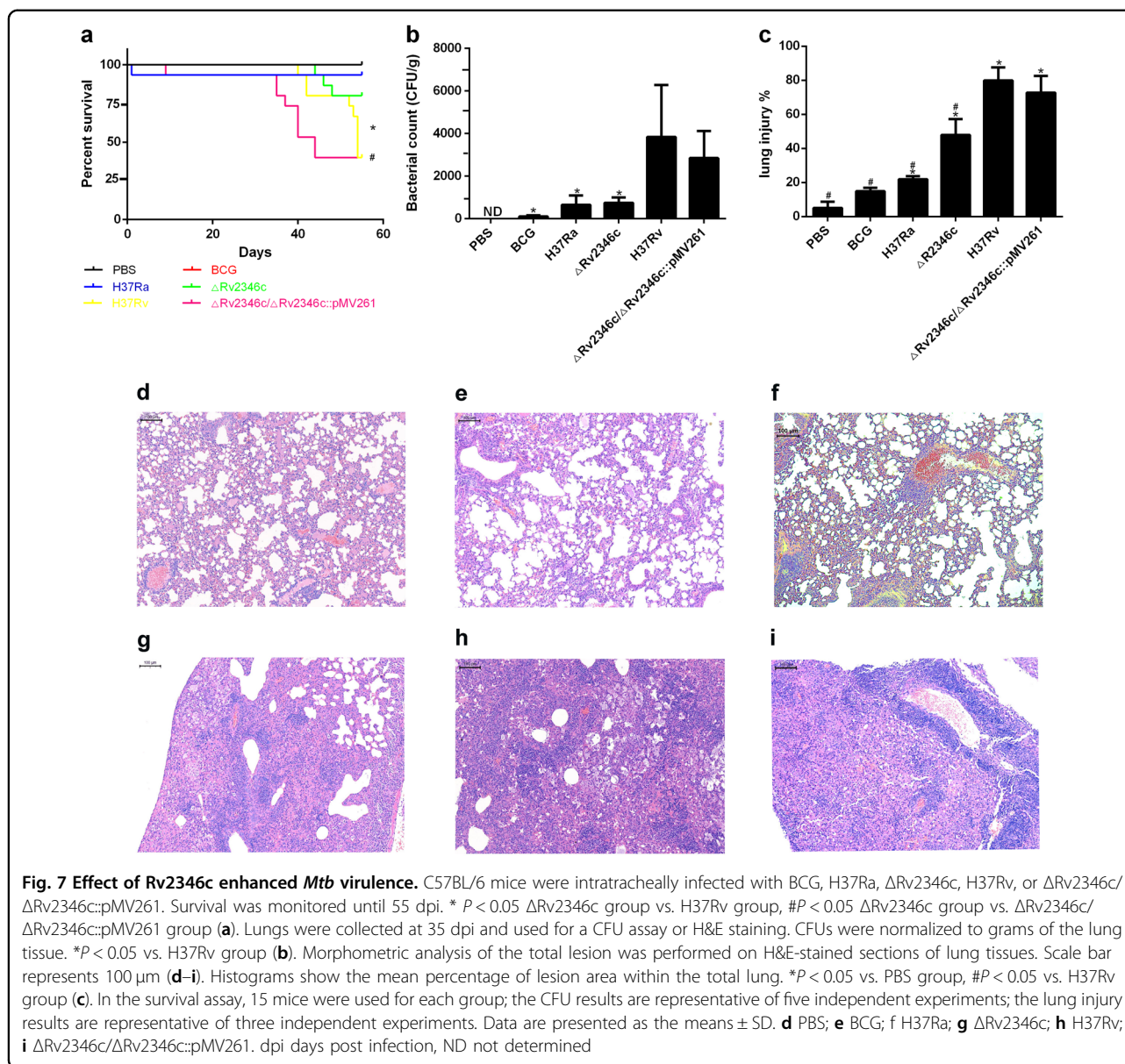
amounts of macrophages infiltrated in the lungs and released greater levels of cytokines (TNF- $\alpha$  and IL-6) compared with mice treated with PBS (Fig. 8). In addition, the fluorescence intensity of TNF- $\alpha$  and IL-6 from mice treated with  $\Delta$ Rv2346c was higher than that observed from H37Rv-treated mice, indicating Rv2346c has a suppressive effect on the production of these cytokines, in accordance with the in vitro results.

## Discussion

Different genomic regions have been identified between virulent *Mtb* and avirulent BCG. A proteomic analysis of *Mtb* and BCG strains identified 13 and 8 unique proteins in *Mtb* H37Rv and BCG, respectively. Identifying differences in protein composition between virulent *Mtb* and attenuated vaccine strains is useful in the discovery of virulence factors and the development of targeted therapies<sup>20</sup>. Rv2346c, an ESAT-6-like protein, is only conserved

in virulent *Mtb* strains and has been shown to promote bacterial persistence inside macrophages<sup>14</sup>. In this study, recombinant Rv2346c protein was produced by DNA template synthesis, PCR amplification, expression vector construction, and protein extraction and purification. The synthetic Rv2346c protein was verified by gene sequencing and western blot analyses and was subsequently used to investigate its importance in *Mtb* infection.

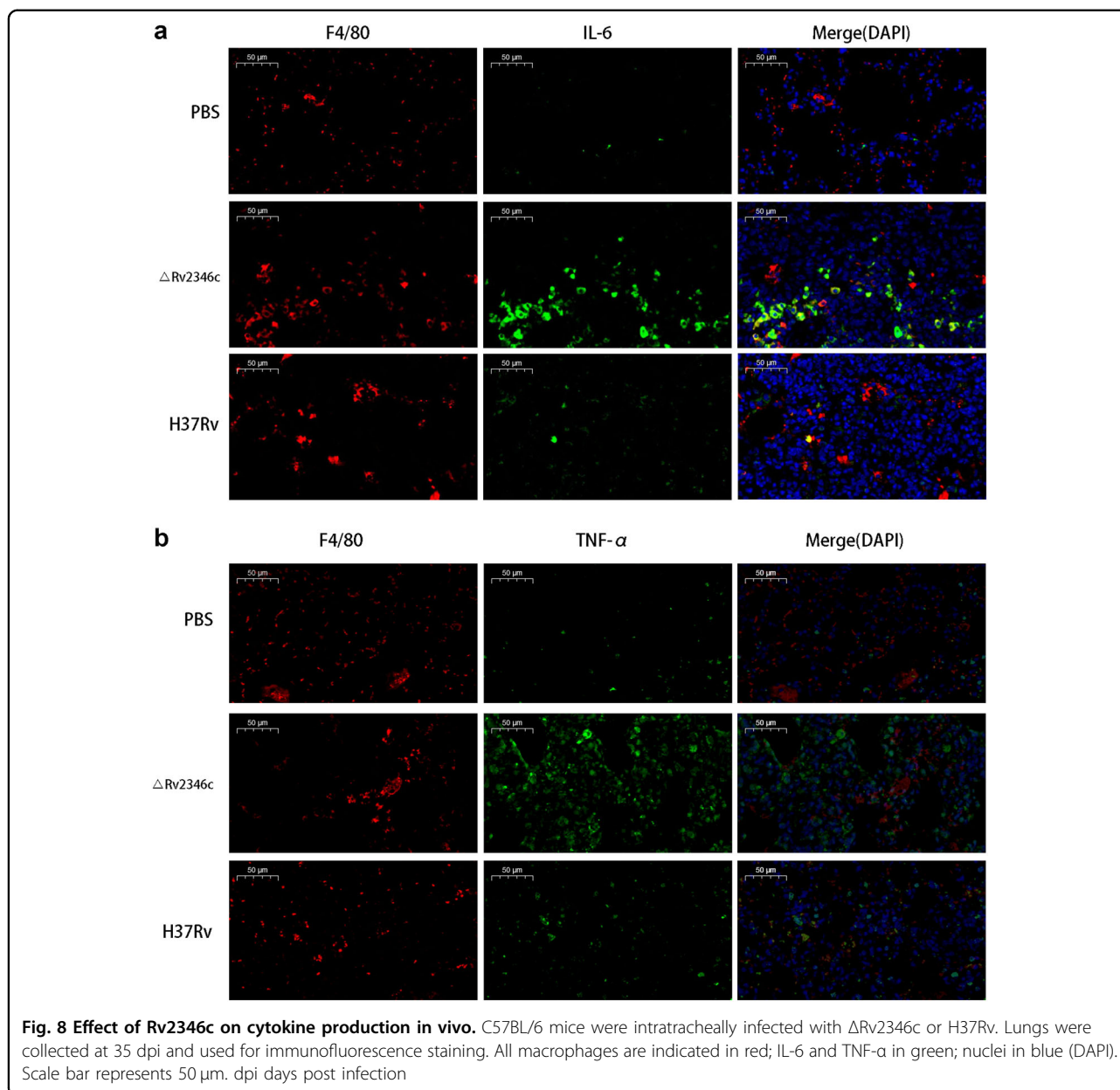
When transmitted via aerosolized droplets, its typical mode of transmission, *Mtb* is phagocytized by alveolar macrophages. Macrophages are considered to be the primary cell population on the frontline of host defenses<sup>21</sup>. Macrophages phagocytize mycobacteria by recognizing specific mycobacterial ligands, resulting in the subsequent activation of antimicrobial pathways. In turn, *Mtb* attempts to counteract the bactericidal activities of the host immunity and establish a niche for long-term survival within macrophages<sup>4,22</sup>. Human monocytic



leukemia U937 cells and murine macrophage RAW264.7 cells infected with BCG were used to evaluate *Mtb* infection and were treated with recombinant Rv2346c protein to assess its function in *Mtb* pathogenesis. The results showed that Rv2346c inhibited the proliferation of BCG-infected macrophages and increased the survival of BCG in macrophages. Moreover, Rv2346c increased the survival of *Mtb* in vivo and aggravated lung injury. These observations indicate that Rv2346c may act as a virulence factor in *Mtb* infection.

TNF- $\alpha$  has a crucial role in the initial and long-term control of TB. Macrophages are induced to secrete TNF- $\alpha$  upon recognizing mycobacterial cell wall components. TNF- $\alpha$  subsequently activates macrophages, recruits them

to the site of infection and participates in granuloma formation<sup>23</sup>. TNF- $\alpha$  secretion by *Mtb*-infected macrophages upregulates nitric oxide synthase 2 expression and induces the production of reactive nitrogen intermediates within phagolysosomes, mediating intracellular *Mtb* killing<sup>15,24</sup>. Neutralization of TNF- $\alpha$  leads to an increased susceptibility to TB and a lack of control of initial or chronic infections<sup>23</sup>. Mice deficient in TNF- $\alpha$  are susceptible to *Mtb* infection<sup>25</sup>. IL-6 also has a crucial role in protecting against *Mtb*, as infection with *Mtb* was observed to be lethal in IL-6-deficient mice<sup>26</sup>. Interestingly, a hypervirulent *Mtb* strain was shown to reduce the levels of proinflammatory cytokines, including TNF- $\alpha$  and IL-6<sup>27</sup>. In our study, the levels of TNF- $\alpha$  and IL-6 were



upregulated in the supernatant of BCG-infected macrophages and were suppressed by Rv2346c, both in vitro and in vivo, consistent with the observed effect of Rv2346c on BCG survival.

The transcription factor NF-κB is essential for the induction expression of a variety of inflammatory genes in response to a range of pathogens and inflammatory cytokines. TNF-α is regulated by the NF-κB signaling pathway in the process of restricting bacterial survival in granulomas and aggregating bacteria and immune cells within the lung. NF-κB in resting cells remains latent in the cytoplasm by binding to IκB proteins. Binding of TNF to TNF receptor type1 leads to activation of the IκB kinase

(IKK) and IKK-mediated phosphorylation of IκB proteins, which results in ubiquitination and proteasome-mediated degradation of IκB. This effect mediates the translocation of the p65 subunit of NF-κB, the accumulation of free NF-κB in the nucleus and induces the transcription of target genes. TNF-α is also included in these targeted genes<sup>17,28</sup>. In addition, IL-6 is reported to be induced in *Mtb*-infected macrophages through NF-κB activation<sup>29</sup>. The results showed that the transcriptional and translational expression of p65 increased during BCG infection and was inhibited by treatment with Rv2346c, indicating that p65 may be the signal molecule modulated by Rv2346c to inhibit the bactericidal activity of macrophages. This

hypothesis was validated by the results obtained from the overexpression and knockdown of p65 in BCG-infected macrophages.

miRNAs are small non-coding endogenous RNA molecules that can regulate a wide range of biological processes via posttranscriptionally regulating gene expression. We performed a microarray assay to identify miRNAs associated with the process of BCG infection and that were affected by the Rv2346c treatment. In the microarray assay, miR-155 and miR-99b were the only miRNAs exhibiting a greater than twofold increase in both RAW264.7 and U937 cells after treatment with Rv2346c during BCG infection. These miRNAs have also been reported to affect the production of cytokines associated with *Mtb* infection. miR-155 has been confirmed as a multifunctional miRNA involved in a variety of biological processes, including infection, inflammation and immunity<sup>9,30</sup>. Dysregulation of miR-155 has been reported in human macrophages that are infected by different *Mycobacterium* species<sup>9</sup>. miR-155 has been reported to be the most highly expressed miRNA in murine macrophages and bone marrow-derived macrophages upon *Mtb* infection<sup>31,32</sup>. Furthermore, miR-155 is associated with TNF- $\alpha$  and IL-6 production<sup>32,33</sup>. The expression of another miRNA, miR-99b, has been reported to result in significant reductions in *Mtb* loads and notable upregulation of proinflammatory cytokines, such as TNF- $\alpha$  and IL-6, when its expression is blocked<sup>32,34</sup>. However, the mechanism underlying this miRNA-mediated effect remains to be determined. To identify miRNAs associated with *Mtb* infection, a microarray assay was performed using BCG-infected macrophages. The results showed that levels of miR-155 and miR-99b were significantly higher in BCG-infected macrophages treated with Rv2346c compared with untreated cells. The results of a qRT-PCR showed that miR-155 and miR-99b were upregulated in macrophages infected with BCG, which were further increased in cells treated with Rv2346c. Further investigation suggested that miR-155 and miR-99b inhibited the expression of p65 and cytokine production, and that a miR-155-binding site is present in the P65-UTR, indicating that miR-155 and miR-99b are negative regulators of p65.

Previous studies have shown that mycobacterial infection acts through TLRs to trigger MAPK pathways, leading to activation of transcription factors, including NF- $\kappa$ B<sup>35,36</sup>. TNF- $\alpha$  production was shown to be induced through a signaling pathway that requires activation of p38 MAPKs in *Mtb*-infected macrophages<sup>37,38</sup>. In addition, a TLR2 or TLR4 deficiency suppressed the activation of p38 and NF- $\kappa$ B, and negatively regulated IL-6 synthesis in H37Rv-infected neutrophils<sup>39</sup>. Activation of p38 and NF- $\kappa$ B mediates IL-6 production in macrophages<sup>40</sup>. However, it was also reported that the inhibition of p38 in

macrophages increases the expression of TNF- $\alpha$  and IL-6<sup>41</sup>. The results of the present study showed that the phosphorylation of p38 was upregulated due to BCG infection, indicating that p38 activation promotes anti-bacterial activity in macrophages. However, p38 phosphorylation was further augmented during Rv2346c intervention, the role of p38 activation during BCG infections is complex and unclear. Further investigation revealed that p38 upregulated the levels of miR-155 and miR-99b, and inhibited the expression of p65 and cytokine production, although changes in p65, miR-155, and miR-99b expression did not notably affect p38 phosphorylation. Thus, we speculate that p38 acts as a positive regulator upstream of miR-155 and miR-99b.

According to our results, we conclude that macrophages produce TNF- $\alpha$  and IL-6 to mediate killing of BCG through activation of NF- $\kappa$ B. Rv2346c suppress the secretion of TNF- $\alpha$  and IL-6, and facilitates the survival of BCG through the p38/miR-155 and miR-99b/NF- $\kappa$ B-pathways. The results of this investigation suggest that Rv2346c acts as a crucial virulence factor during *Mtb* infection and has potential use as a target for anti-TB therapy.

## Materials and methods

### Production of recombinant Rv2346c protein

A DNA fragment encoding Rv2346c was obtained from GenScript (Nanjing, China) and the oligonucleotide primers were designed with Primer 5.0 (Premier, Canada) (Table S1). The DNA template and primers were synthesized by GenScript and PCR was performed with the template described above. The thermocycling program used was as follows: 94 °C for 5 min, followed by 30 cycles of 96 °C for 25 s, 58 °C for 25 s, and 72 °C for 1 min. The PCR product was cut and purified via DNA gel extraction kit (AXYGEN, NY, USA). The purified PCR product and pET-30a(+) (Novagen, Germany) were digested with NdeI and HindIII (NEB) (Thermo Scientific, DE, USA) and ligated together with T4 DNA ligase (Thermo Scientific). The pET-30a(+) vector containing the Rv2346c-encoding gene was transformed by electroporation into *E. coli* strain BL21(DE3) (Novagen) and the cells were subsequently grown on Luria-Bertani (LB) agar plates containing 50  $\mu$ g/ml kanamycin at 37 °C overnight. The positive clones were selected and confirmed by sequencing. The confirmed plasmids were transformed into *E. coli* BL21(DE3) and plated onto solid medium, after which a single colony was selected and cultivated in LB medium in a shaking incubator. When the OD<sub>600</sub> reached 0.6, cells were induced with isopropyl- $\beta$ -D-thiogalactoside (1 mmol/L). Next, the culture was centrifuged and cells were resuspended and lysed by sonication. The sonicated sample was centrifuged and the supernatant of the cell lysate was applied to a Ni-IDA resin (GenScript). The

protein was subsequently eluted and the eluate was collected for SDS-polyacrylamide gel electrophoresis analysis. A protein with the predicted mass of Rv2346c was concentrated through ultrafiltration (molecular weight cutoff 10 kDa). The concentration of the protein was determined by the Bradford method. Subsequently, a western blotting was performed to examine the purified recombinant Rv2346c protein via the N-His Tag (His Tag antibody; GenScript).

#### Cell culture

U937 cells (American Type Culture Collection (ATCC), Manassas, VA, USA), a human monocytic leukemia cell line, were cultured in RPMI-1640 medium (Gibco BRL, Grand Island, NY, USA) supplemented with 10% fetal bovine serum (FBS, Gibco BRL), penicillin (100 U/ml), streptomycin (100 µg/ml), and L-glutamine (2 mM), and were maintained at 37 °C under a humidified atmosphere containing 5% CO<sub>2</sub>.

RAW264.7 cells (ATCC), a murine macrophage cell line, were cultured in DMEM medium (Gibco BRL) supplemented with 10% FBS, penicillin (100 U/ml), streptomycin (100 µg/ml), and L-glutamine (2 mM), and were maintained at 37 °C under a humidified atmosphere containing 5% CO<sub>2</sub>.

#### Bacterial culture

The BCG Beijing strain developed from BCG Denmark was provided by the Jiangsu Provincial Center for Disease Control and Prevention. BCG was grown on Sauton's medium. After culturing for 3 weeks, bacteria were collected and resuspended in cell culture medium without antibiotics. The solution was adjusted to an OD<sub>600</sub> of 0.5 (~10<sup>7</sup> bacteria/ml). The bacterial suspension was used to infect cells at the indicated MOI.

*Mtb* H37Rv (ATCC, no.27294), H37Ra (ATCC, no.25177), the Rv2346c-deleted strain ( $\Delta$ Rv2346c) (Shanghai Gene-optimal Science & Technology, Shanghai, China) and the Rv2346c-gene complemented strain ( $\Delta$ Rv2346c/ $\Delta$ Rv2346c::pMV261) (Shanghai Gene-optimal Science & Technology) were grown in Middlebrook 7H9 broth (Difco, Detroit, MI, USA) supplemented with 0.2% glycerol, 0.05% Tween 80, and 10% Middlebrook OADC for 4–6 weeks. Mid-log phase cultures were harvested and stored at –80 °C. Before infecting animals, stock solutions of *Mtb* were thawed, washed, and diluted in sterile distilled water to a specific concentration.

#### Transfection

The fragments encoding the sequences of the p65 and p38 alleles were obtained from GenScript and cloned into pcDNA3.1 (Invitrogen, Carlsbad, CA, USA). U937 and RAW264.7 cells were transiently transfected with pcDNA3.1/p65 cDNA, pcDNA3.1/p38 cDNA, control

pcDNA3.1, miR-155 mimic (GenePharma, Shanghai, China), miR-99b mimic (GenePharma), or a negative control (NC) miRNA (GenePharma) using Lipofectamine 3000 (Invitrogen) according to the manufacturer's instructions. A control pcDNA3.1 or an NC miRNA was used as a NC. Cells were incubated for 24 h at 37 °C before being used for further analysis.

siRNAs targeting NF- $\kappa$ B p65 subunit mRNA or p38 mRNA, a random non-coding siRNA, a miR-155 inhibitor, a miR-99b inhibitor and an NC mRNA were synthesized by GenePharma. U937 and RAW264.7 cells were transfected with the above siRNAs or miRNAs using Lipofectamine 3000 according to the manufacturer's instructions. A non-coding siRNA or an NC miRNA was used as a NC. The cells were exposed to BCG and recombinant Rv2346c protein at 24 h post transfection for additional assays. The corresponding sequences of these RNAs are shown in Table S2.

#### Proliferation assay

U937 or RAW264.7 cells were seeded at 5000 cells per well in 96-well plates. After incubating overnight, the BCG-infected groups were infected with BCG at the indicated MOIs (cell/bacillus: 1/1, 1/5, 1/10, 1/50). The BCG + Rv2346c groups were infected with BCG (MOI: 1/5) and treated with Rv2346c at the indicated concentrations (50, 100, 500, and 1000 pg/ml). For the control group, cells were treated with an equal volume of medium. The final volume was adjusted to 100 µl per well. After incubating for 24, 48, 72, or 96 h, the proliferation assay was performed using a CCK-8 kit (Dojindo Laboratories, Kumamoto, Japan) according to the manufacturer's protocol.

#### Bacterial enumeration

U937 or RAW264.7 cells were plated in 24-well plates (1 × 10<sup>5</sup> cells per well) and cultured overnight. Cells in the BCG-infected group were infected with BCG (MOI: 1/5), whereas cells in the BCG + Rv2346c group were infected with BCG (MOI 1/5) and treated with recombinant Rv2346c protein (500 pg/ml). Cells were washed with warm phosphate-buffered saline after 4 h to remove non-ingested mycobacteria. Subsequently, after incubating for 24, 48, or 72 h, the infected cells were washed and lysed. The lysates were serially diluted (1:100), and 100 µl of the suspensions were plated on Sauton's medium. CFUs was counted after incubation at 37 °C for 4 weeks.

#### ELISA assay

Cell-free supernatants were collected and used to evaluate the concentrations of TNF- $\alpha$  and IL-6 with a human TNF- $\alpha$  ELISA kit (R&D Systems, Minneapolis, MN, USA), a human IL-6 ELISA kit (R&D Systems), a mouse TNF- $\alpha$  ELISA kit (R&D Systems), and a mouse IL-6

ELISA kit (R&D Systems) according to the manufacturer's instructions.

#### Western blotting

U937 and RAW264.7 cells were infected with BCG (MOI 1/5) and cells in the BCG + Rv2346c groups were treated with Rv2346c (500 pg/ml). After incubating for 24, 48, or 72 h, the cells were collected and lysed. The lysates were centrifuged, denatured, applied to an SDS-polyacrylamide gel for electrophoresis and transferred to a polyvinylidene fluoride membrane. The membranes were then blocked with 5% non-fat dry milk at room temperature for 1 h, followed by an incubation with primary antibodies at 4 °C overnight. The primary antibodies included an anti-NF- $\kappa$ B p65 (Abcam, MA, USA), an anti-NF- $\kappa$ B p65 (phospho S536) antibody (Abcam), an anti-p38 antibody (Abcam), an anti-p38 (phospho Y182) antibody (Abcam), and an anti-glyceraldehyde-phosphate dehydrogenase (GAPDH) antibody (Abcam). After washing, the membranes were incubated with the appropriate horseradish peroxidase-conjugated secondary antibody at room temperature for 2 h. The results were visualized via chemiluminescence using an ECL kit (Thermo scientific) and photographed with a Tanon MultiImager. The density of the immunoreactive bands was measured using ImageJ; GAPDH was used as an internal control.

#### Microarray data analysis

U937 or RAW264.7 cells were infected with BCG (MOI 1/5) with or without the Rv2346c (500 pg/ml) treatment. After incubating for 24 h, cells were collected for total RNA extraction. RNA labeling was performed with a miRNA Complete Labeling and Hyb Kit (Agilent Technologies, Santa Clara, CA, USA) according to the manufacturer's protocol. Each slide was hybridized with 100 ng of Cy3-labeled RNA in a hybridization oven set at 55 °C, 20 r.p.m. for 20 h. After hybridization, slides were washed in staining dishes with a Gene Expression Wash Buffer Kit (Agilent Technologies), scanned by an Agilent Microarray Scanner, and analyzed using Feature Extraction 10.7 (Agilent Technologies). Raw data were normalized by a Quantile algorithm using Gene Spring 12.6 (Agilent Technologies). The pairwise expression fold change was calculated after merging the spots with same Agilent probe ID (Agilent Human miRNA (8\*60 K) V19.0, design ID: 46064; Agilent Mouse miRNA (8\*60 K), design ID:58698). Differentially expressed genes were defined as those exhibiting a |fold change| > 2.

#### Quantitative RT-PCR

U937 and RAW264.7 cells were infected with BCG (MOI 1/5) with or without the Rv2346c (500 pg/ml) treatment. After incubating for 24, 48, or 72 h, total RNA

was extracted from the cells using a Total RNA Extraction Kit (Generay Biotech, Shanghai, China). gDNA ERASER (Takara, Shiga, Japan) was used to eliminate DNA when extracting RNA. RNA was reverse-transcribed into cDNA using a RevertAid First Strand cDNA synthesis Kit (Thermo Scientific Fisher, Waltham, MA, UK) and the thermocycling program used was as follows: 37 °C for 60 min and 85 °C for 5 min. Amplification was conducted using a Stepone plus Real-Time System with a SYBR Premix ExTM Taq (Tli RNaseH Plus) Kit (TaKaRa, Tokyo, Japan) under the following thermocycling conditions: 50 °C for 3 min and 95 °C for 15 min, followed by 40 cycles of 95 °C for 10 s, 60 °C for 20 s, and 72 °C for 30 s. mRNA expression was calculated using the  $2^{-\Delta\Delta C_t}$  method. All values were normalized to the housekeeping gene GAPDH. The PCR primers used are listed in Table S1.

Total RNA for miR-99b, miR-155, and U6 detection was extracted with a Total RNA Extraction Kit. Reverse transcription and PCR was performed using a Bulge-Loop<sup>TM</sup> miRNA qRT-PCR Starter Kit, a Bulge-Loop<sup>TM</sup> miRNA qRT-PCR Primer Set, and a U6 snRNA qPCR Primer Set (RiboBio, Guangzhou, China) according to the manufacturer's instructions. miRNA expression was quantified using the  $2^{-\Delta\Delta C_t}$  method. U6 was used as an internal control.

#### Dual-luciferase reporter assay

The wild-type (WT) and mutant (MUT) 3'-untranslated region (3'-UTR) fragment of p65 (human/mouse) was inserted into the pGL3-basic vector (firefly luciferase; Promega, Madison, WI, USA), which was obtained from General Biosystems (Anhui, China). U937 or RAW264.7 cells were co-transfected with p65-UTR-WT or p65-UTR-MUT plasmids along with miR-155 or miR-99b mimics or scramble oligonucleotides using Lipofectamine 3000. A reporter vector carrying the WT or MUT sequences of p65-UTR was assayed for luciferase expression using the Dual-Luciferase<sup>®</sup> Reporter Assay System (Promega) following the manufacturer's instructions. For data analysis, firefly luciferase activity was normalized to the corresponding *Renilla* luciferase activity.

#### Infection of mice

Six- to 8-week-old female C57BL/6 mice (Cavens Lab Animal Company, Changzhou, China) were housed in a bio-safety level III animal facility under specific pathogen-free conditions. All animal experimental procedures were approved by the Institutional Animal Ethics Committee of the Second Affiliated Hospital of Nanjing Medical University (No.2014KY050) and were carried out in strict accordance with the Nanjing Medical University's guidelines for their care and use. Mice were anesthetized using

an intraperitoneal injection of 4% chloral hydrate and were inoculated intratracheally with each *Mycobacterium* strain at a dose of  $2 \times 10^6$  CFU per mouse. The survival of mice was monitored daily from the day of infection to 55 dpi.

### Bacterial load assessment in the lung

To determine the bacterial loads in the lungs, the mice were killed at 35 dpi. Lungs were removed aseptically, weighed, and homogenized. Serial dilutions of tissue homogenates were plated onto Middlebrook 7H11 agar. Bacterial CFUs were enumerated after 4–6 weeks of incubation at 37 °C.

### Histology examination

Lung lobes were collected at 35 dpi, fixed with 4% paraformaldehyde overnight, and embedded in paraffin. H&E-stained tissues were assessed via a pathology analysis. Lung injury was estimated by the percentage of the lesion area in the total lung area using an ImagePro macro.

### Immunofluorescence detection

Immunofluorescence detection of TNF- $\alpha$  and IL-6 was performed using tissue sections that were dewaxed and rehydrated. Antigen retrieval was performed using a proteinase K and hot citric acid buffer treatment as needed. The restored sections were incubated with primary antibodies overnight at 4 °C, including anti-F4/80 (Abcam), anti-TNF- $\alpha$  (Abcam), and anti-IL-6 (Abcam) antibodies. Macrophages were observed using an F4/80 antigen. Next, tissue sections were stained with Alexa Fluor® 488-conjugated or Alexa Fluor® 647-conjugated secondary antibodies (Abcam) for 1 h at room temperature and mounted with SlowFade® Gold Antifade with 4',6-diamidino-2-phenylindole (Invitrogen). Images were taken with a Leica Microsystems Ltd microscope and were analyzed using ImagePro Plus 6.

### Statistical analysis

All the presented results were confirmed in three independent experiments. The Student's *t*-test was used to compare two groups and one-way analysis of variance followed by Least Significant Difference (LSD) was used to compare multiple groups. Survival curves was analyzed using the Log-rank test. Statistical analyses were performed using SPSS 20.0 (IBM SPSS, Armonk, NY, USA).  $P < 0.05$  was considered to be significantly different.

### Data availability

All data generated or analyzed during this study are included in this published article (and its Supplementary Information files).

### Acknowledgements

This work was supported by grant from Natural Science Foundation of China (number 81470209).

### Author details

<sup>1</sup>Department of Respiratory Medicine, the Second Affiliated Hospital of Nanjing Medical University, Nanjing, Jiangsu 210011, China. <sup>2</sup>Department of Infectious Diseases, the Second Affiliated Hospital of Nanjing Medical University, Nanjing, Jiangsu 210011, China. <sup>3</sup>Jiangsu Provincial Center for Disease Control and Prevention, Nanjing, Jiangsu 210009, China. <sup>4</sup>Department of Respiratory Medicine, the First People's Hospital of Kunshan, Kunshan, Jiangsu 215300, China. <sup>5</sup>Department of Respiratory Medicine, Sir Run Run Hospital, Nanjing, Jiangsu 211100, China

### Conflict of interest

The authors declare no conflicts of interest.

### Publisher's note

Springer Nature remains neutral with regard to jurisdictional claims in published maps and institutional affiliations.

**Supplementary Information** accompanies this paper at (<https://doi.org/10.1038/s41426-018-0162-6>).

Received: 16 April 2018 Revised: 15 August 2018 Accepted: 20 August 2018

Published online: 19 September 2018

### References

- O'Garra, A. et al. The immune response in tuberculosis. *Annu. Rev. Immunol.* **31**, 475–527 (2013).
- Matsuo, K. & Yasutomi, Y. *Mycobacterium bovis* Bacille Calmette-Guerin as a vaccine vector for global infectious disease control. *Tuberc. Res. Treat.* **2011**, 574591 (2011).
- Nieuwenhuizen, N. E. et al. The recombinant Bacille Calmette-Guerin vaccine VPM1002: ready for clinical efficacy testing. *Front. Immunol.* **8**, 1147 (2017).
- Xu, G., Wang, J., Gao, G. F. & Liu, C. H. Insights into battles between *Mycobacterium tuberculosis* and macrophages. *Protein Cell* **5**, 728–736 (2014).
- Underhill, D. M., Ozinsky, A., Smith, K. D. & Aderem, A. Toll-like receptor-2 mediates mycobacteria-induced proinflammatory signaling in macrophages. *Proc. Natl Acad. Sci. USA* **96**, 14459–14463 (1999).
- Flynn, J. L. & Chan, J. Immunology of tuberculosis. *Annu. Rev. Immunol.* **19**, 93–129 (2001).
- Kundu, M. et al. A TNF- and c-Cbl-dependent FLIP(S)-degradation pathway and its function in *Mycobacterium tuberculosis*-induced macrophage apoptosis. *Nat. Immunol.* **10**, 918–926 (2009).
- Martinez, A. N., Mehra, S. & Kaushal, D. Role of interleukin 6 in innate immunity to *Mycobacterium tuberculosis* infection. *J. Infect. Dis.* **207**, 1253–1261 (2013).
- Harapan, H. et al. The roles of microRNAs on tuberculosis infection: meaning or myth? *Tuberc. (Edinb.)* **93**, 596–605 (2013).
- Samten, B., Wang, X. & Barnes, P. F. *Mycobacterium tuberculosis* ESX-1 system-secreted protein ESAT-6 but not CFP10 inhibits human T-cell immune responses. *Tuberculosis (Edinb.)* **89**(Suppl 1), S74–S76 (2009).
- Manzanillo, P. S., Shiloh, M. U., Portnoy, D. A. & Cox, J. S. *Mycobacterium tuberculosis* activates the DNA-dependent cytosolic surveillance pathway within macrophages. *Cell Host Microbe* **11**, 469–480 (2012).
- Simeone, R. et al. Phagosomal rupture by *Mycobacterium tuberculosis* results in toxicity and host cell death. *PLoS Pathog.* **8**, e1002507 (2012).
- Mahairas, G. G., Sabo, P. J., Hickey, M. J., Singh, D. C. & Stover, C. K. Molecular analysis of genetic differences between *Mycobacterium bovis* BCG and virulent *M. bovis*. *J. Bacteriol.* **178**, 1274–1282 (1996).
- Mohanty, S. et al. *Mycobacterium tuberculosis* EsxO (Rv2346c) promotes bacillary survival by inducing oxidative stress mediated genomic instability in macrophages. *Tuberculosis (Edinb.)* **96**, 44–57 (2016).
- Hossain, M. M. & Norazmi, M. N. Pattern recognition receptors and cytokines in *Mycobacterium tuberculosis* infection—the double-edged sword? *Biomed. Res. Int.* **2013**, 179174 (2013).

16. Maturi, A., Maggi, E. & Vultaggio, A. Cellular and humoral immune responses during tuberculosis infection: useful knowledge in the era of biological agents. *J. Rheumatol. Suppl.* **91**, 17–23 (2014).
17. Zhao, W. et al. *Mycobacterium bovis* ornithine carbamoyltransferase, MB1684, induces proinflammatory cytokine gene expression by activating NF-kappaB in macrophages. *DNA Cell Biol.* **33**, 311–319 (2014).
18. Gasparini, C. & Feldmann, M. NF-kappaB as a target for modulating inflammatory responses. *Curr. Pharm. Des.* **18**, 5735–5745 (2012).
19. Cho, S. S. L. et al. Dual-specificity phosphatase 12 targets p38 MAP kinase to regulate macrophage response to intracellular bacterial infection. *Front. Immunol.* **8**, 1259 (2017).
20. Jungblut, P. R. et al. Comparative proteome analysis of *Mycobacterium tuberculosis* and *Mycobacterium bovis* BCG strains: towards functional genomics of microbial pathogens. *Mol. Microbiol.* **33**, 1103–1117 (1999).
21. Amaral, E. P., Lasunskia, E. B. & D'Imperio-Lima, M. R. Innate immunity in tuberculosis: how the sensing of mycobacteria and tissue damage modulates macrophage death. *Microbes Infect.* **18**, 11–20 (2016).
22. Sia, J. K., Georgieva, M. & Rengarajan, J. Innate immune defenses in human tuberculosis: an overview of the interactions between *Mycobacterium tuberculosis* and innate immune cells. *J. Immunol. Res.* **2015**, 747543 (2015).
23. Lin, P. L., Plessner, H. L., Voitenok, N. N. & Flynn, J. L. Tumor necrosis factor and tuberculosis. *J. Invest. Dermatol. Symp. Proc.* **12**, 22–25 (2007).
24. Flynn, J. L. & Chan, J. Immune evasion by *Mycobacterium tuberculosis*: living with the enemy. *Curr. Opin. Immunol.* **15**, 450–455 (2003).
25. Torrado, E. & Cooper, A. M. Cytokines in the balance of protection and pathology during mycobacterial infections. *Adv. Exp. Med. Biol.* **783**, 121–140 (2013).
26. Ladel, C. H. et al. Lethal tuberculosis in interleukin-6-deficient mutant mice. *Infect. Immun.* **65**, 4843–4849 (1997).
27. Reed, M. B. et al. A glycolipid of hypervirulent tuberculosis strains that inhibits the innate immune response. *Nature* **431**, 84–87 (2004).
28. Fallahi-Sichani, M., Kirschner, D. E. & Linderman, J. J. NF-kappaB signaling dynamics play a key role in infection control in tuberculosis. *Front. Physiol.* **3**, 170 (2012).
29. Li, H., Li, Q., Yu, Z., Zhou, M. & Xie, J. *Mycobacterium tuberculosis* PE13 (Rv1195) manipulates the host cell fate via p38-ERK-NF-kappaB axis and apoptosis. *Apoptosis* **21**, 795–808 (2016).
30. Tsiou, E. & Lindsay, M. A. MicroRNAs and the immune response. *Curr. Opin. Pharmacol.* **9**, 514–520 (2009).
31. Brook, M. et al. Posttranslational regulation of tristetraprolin subcellular localization and protein stability by p38 mitogen-activated protein kinase and extracellular signal-regulated kinase pathways. *Mol. Cell Biol.* **26**, 2408–2418 (2006).
32. Abdalla, A. E., Duan, X., Deng, W., Zeng, J. & Xie, J. MicroRNAs play big roles in modulating macrophages response toward mycobacteria infection. *Infect. Genet. Evol.* **45**, 378–382 (2016).
33. Rajaram, M. V. et al. *Mycobacterium tuberculosis* lipomannan blocks TNF biosynthesis by regulating macrophage MAPK-activated protein kinase 2 (MK2) and microRNA miR-125b. *Proc. Natl Acad. Sci. USA* **108**, 17408–17413 (2011).
34. Singh, Y. et al. *Mycobacterium tuberculosis* controls microRNA-99b (miR-99b) expression in infected murine dendritic cells to modulate host immunity. *J. Biol. Chem.* **288**, 5056–5061 (2013).
35. Kim, K. H. et al. Mycobacterial heparin-binding hemagglutinin antigen activates inflammatory responses through PI3-K/Akt, NF-kappaB, and MAPK pathways. *Immune Netw.* **11**, 123–133 (2011).
36. Wang, C. H. et al. Heat shock protein70 is implicated in modulating NF-kappaB activation in alveolar macrophages of patients with active pulmonary tuberculosis. *Sci. Rep.* **7**, 1214 (2017).
37. Torres-Huerta, A. et al. Interaction of the CD43 sialomucin with the *Mycobacterium tuberculosis* Cpn60.2 chaperonin leads to tumor necrosis factor alpha production. *Infect. Immun.* **85**, <https://doi.org/10.1128/IAI.00915-16> (2017).
38. Li, W. et al. *Mycobacterium tuberculosis* Rv3402c enhances mycobacterial survival within macrophages and modulates the host pro-inflammatory cytokines production via NF-kappa B/ERK/p38 signaling. *PLoS ONE* **9**, e94418 (2014).
39. Hu, S. et al. IL-17 production of neutrophils enhances antibacteria ability but promotes arthritis development during *Mycobacterium tuberculosis* infection. *EBioMedicine* **23**, 88–99 (2017).
40. Iwasaki, A. & Medzhitov, R. Toll-like receptor control of the adaptive immune responses. *Nat. Immunol.* **5**, 987–995 (2004).
41. van den Blink, B. et al. p38 mitogen-activated protein kinase inhibition increases cytokine release by macrophages in vitro and during infection in vivo. *J. Immunol.* **166**, 582–587 (2001).